

J.Serb.Chem.Soc. 66(11–12)923–933(2001)
JSCS –2915

UDC 539.24+531.755+543:669–492.2/.3+669.3
Original scientific paper

The effect of particle structure on apparent density of electrolytic copper powder*

M. G. PAVLOVIĆ^{1#}, L.J. J. PAVLOVIĆ¹, E. R. IVANOVIĆ², V. RADMILOVIĆ³ and
K. I. POPOV^{3#}

¹*ICTM - Department of Electrochemistry, Njegoševa 12, YU-11000 Belgrade,* ²*Faculty of Agriculture, University of Belgrade, Nemanjina 6, YU-11080 Zemun - Belgrade and* ³*Faculty of Technology and Metallurgy, University of Belgrade, Karnegijeva 4, YU-11000 Belgrade, Yugoslavia*

(Received 6 June, revised 30 August 2001)

The quantitative microstructural analysis and the sieve analysis of copper powder as well as the scanning electron microscopy analysis of the copper powders particles were performed. It was found that the structure of the copper powder particles determines the apparent density of copper powder. The powder particles from the same fractions of different powders occupy approximately the same volume, but the structure of metallic copper is very different. This causes the difference in apparent densities of copper powder obtained under different conditions. The more dendritic is the structure of powder particles the smaller is the apparent density of copper powder.

Keywords: particle structure, apparent density, electrolytic copper powder, galvanostatic deposition.

INTRODUCTION

Thanks to a rapid increase in significance of powder metallurgy, metal powders are being produced in large quantities nowadays and a big part is being produced by electrolysis. A powder is defined as a finely divided solid, smaller than 1 mm in its maximum dimensions. An important characteristic of a powder is its relatively high surface area to volume ratio.¹ Depending on the shape of the product, initial powders have to satisfy different requirements. These include physical (size and particle size distribution, state of the surface), chemical (basic metal and admixture content, chemically bonded, adsorbed or dissolved gas contaminants content) and technological properties (bulk weight, flow rate, pressing ability, *etc.*).

The electrolytic powder production method usually allows products of high purity which can well be pressed and sintered. Besides, in recent years it has been shown

* This paper is dedicated to Professor Dragutin M. Dražić on the occasion of his 70th birthday.

Serbian Chemical Society active member.

that by different electrolysis regimes it is possible not only to obtain powders with a wide range of properties but to predict the decisive characteristic of powders which are of vital importance for the powder quality and for the appropriate purpose.²

For metal powder application, a series of their properties are of interest; the size and shape of the particles, the bulk weight, flow rate, the corrosion resistance, the specific surface area, the apparent density and the quality of the sintered products. Finally, the properties mentioned depend on the shape and the size of the particles which can be influenced by electrolysis regimes.^{2,3}

A particle is defined as the smallest unit of a powder that can not be subdivided. Generally, powder metallurgy deals with particles that are larger than smoke (0.01 to 1 μm), but smaller than sand (0.1 to 1 mm). Many metal powders are similar in size to the diameter of a human hair (25 to 200 μm).¹

It is necessary to control the following variables to produce electrolytic powder within a specified range of physical properties. These are: (a) electrolyte composition (acid and copper content); (b) electrolyte temperature; (c) electrolyte circulation rate; (d) current density; (e) size and type of anode and cathode; (f) electrode spacing and (g) time of powder removal. The above variables have strong effects on the apparent density.

According to the production process and the nature of the metal used, differently shaped particles (granules) can be obtained. Shape is identified through direct, naked-eye, magnifying glass, optical or electron scanning microscope observation, according to particle size. The scanning electron microscope (SEM) is one of the best tools available for observing the discrete characteristics of metal powders. However, one of the decisive characteristics of powders is apparent density. (The ratio between the mass and the volume represents the apparent density. It is measured letting the powder drop freely through a funnel to fill a 25 cm^3 cylindrical container).⁴

Apparent density of a metal powder depends on a series of factors, the more important of which are as follows:

- metal true density
- powder shape (the more regular the shape, the denser the powder)
- granulometry (the looser the granule distribution, the higher the density; the more concentrated the distribution, the lower the density; in the case of spherical or rather regularly shaped powders, density gets higher in general when the size gets smaller, whereas in the case of dendritic or foliated powders the finer they are, the lower the density is)
- oxidation level
- granules rugosity and porosity.

There is wide scope for variations *i.e.* spherical copper powder at 5.6 g/cm^3 density (64 % of its true density) may be found, but also dendritic copper powder at 0.5 g/cm^3 density (5.7 % of its true density which is 8.85 g/cm^3).¹

Generally speaking, the larger the powder specific surface the lower its apparent density, and all the more so the smaller the particle size. On the other hand, it seems to be that particle structure has the vital importance on apparent density and on the powder quality.

The purpose of this work was to show the effect of particle structure on apparent density of electrolytic copper powder in galvanostatic deposition in an enlarged electrochemical reactor.

EXPERIMENTAL

The experiments were performed in the enlarged laboratory plastic reactor with a cell volume of 10 dm³. Electrolytic copper powder has been produced from electrolytes containing 140 g/dm³ sulphuric acid and 15 g/dm³ copper, using an electrolyte temperature $(50 \pm 2)^\circ\text{C}$.² The electrolyte circulation system was designed to supply the laboratory scale cell from one electrolyte supply tank (100 dm³).

The enlarged laboratory reactor had a circulation pump, inlet and outlet for the electrolyte and a heat exchanger. The latter controlled the electrolyte temperature. Electrolyte was pumped from basement storage tank to enlarged laboratory reactor; (electrolyte circulation rate: 0.11 dm³/min). From there it flowed by gravity and then into the back and the top of the cell. Thus circulation of electrolyte in the tanks was top to bottom. This yields a finer, more homogeneous powder than bottom to top circulation. Electrolyte returns to the basement storage by gravity.

The cell was loaded with four copper cathodes at a spacing of 30 mm between centers [each holding four vertical copper rods (120 mm long, 8 mm diameter)], and five copper anodes (120×120×10) mm which were hung between the cathodes. The distance between anodes was 60 mm from center to center of each anode. The electrodes in the cell were in parallel with each other.

Electrolytic copper powder was deposited galvanostatically at current densities 1800 A/m² and 3600 A/m².

The electrolytes were prepared from technical chemicals and demineralized water.

The deposition times (times of powder removal by brush) were 15 and 90 min.

The wet powder was washed several times with a large amount of demineralized water until the powder was free from traces of acid, at room temperature; the latter promotes rapid oxidation of the powder during drying. It is essential that washing takes place immediately, so that oxidation of the copper particles is precluded. To inhibit oxidation, benzoic acid, as stabilizer, was added as additive (0.1 %) to water for washing copper powder, to protect the powder against subsequent oxidation.⁵ This substance was removed by further washing.

The powder was then dried in tunnel furnaces in a controlled atmosphere (by nitrogen), at 110 – 120 °C.

Finally, the sieve analysis of granular metal powders was done.⁶

Quantitative microstructural analysis of the copper powder was recorded by Leica Q500 MC ("Reichert-Jung").^{7,8}

The morphology of the deposits was investigated by means of scanning electron microscopy (using a JOEL T20 microscope).

RESULTS AND DISCUSSION

Two kinds of copper powder were obtained under the following conditions:

Powder I: current density, $j = 3600 \text{ A/m}^2$, time of powder removal, $\tau_r = 15 \text{ min}$, electrolyte circulation rate, $Q = 0.11 \text{ dm}^3/\text{min}$, electrolyte temperature, $t = (50 \pm 2)^\circ\text{C}$, concentration of copper, $c(\text{Cu}^{+2}) = 15 \text{ g/dm}^3$ and concentration of H_2SO_4 , $c(\text{H}_2\text{SO}_4) = 140 \text{ g/dm}^3$.

Powder II: $j = 1800 \text{ A/m}^2$, $\tau_r = 1.5 \text{ h}$, $Q = 0.11 \text{ dm}^3/\text{min}$, $t = (50 \pm 2)^\circ\text{C}$, $c(\text{Cu}^{+2}) = 15 \text{ g/dm}^3$ and $c(\text{H}_2\text{SO}_4) = 140 \text{ g/dm}^3$.

The apparent densities of powders I and II were 0.528 and 1.838 g/cm³ respectively, and the results of quantitative microstructural analysis are shown in Tables I and II and Figs. 1–8.

TABLE I. The parameters which characterize powder I (not sieved)

	Min	Max	Mean	RSE/%
Area/ μm^2	8.77	1653.88	318.46	2.55
$D_{\text{max}}/\mu\text{m}$	3.31	100.66	32.33	1.61
$D_{\text{min}}/\mu\text{m}$	1.99	43.71	15.49	1.53
L_p (perimeter)/ μm	11.92	279.47	88.90	1.62
f_A (form area)	9.93	227.81	78.44	1.53
f_R (roundness)	1.12	6.36	2.12	0.95
f_w	0.70	0.97	0.89	0.15
f_L (form perimeter)	0.15	0.84	0.48	0.89

TABLE II. The parameters which characterize powder II (not sieved)

	Min	Max	Mean	RSE/%
Area/ μm^2	8.70	4377.44	654.06	1.83
$D_{\text{max}}/\mu\text{m}$	3.25	154.30	42.13	1.11
$D_{\text{min}}/\mu\text{m}$	1.97	64.90	22.44	1.04
L_p (perimeter)/ μm	11.90	392.05	119.63	1.10
f_A (form area)	9.93	356.29	105.24	1.05
f_R (roundness)	1.07	6.40	1.95	0.61
f_w	0.59	0.97	0.89	0.10
f_L (form perimeter)	0.15	0.88	0.51	0.52

The maximal (max), minimal (min) and average values (mean) of parameters which characterize the metal powders, as well as the maximum relative error (RSE), are presented in Tables I and II and their cumulative frequencies in corresponding Figs. 1–8. The symbols used have the following meanings:

- A (area) – Feature area (the total number of detected pixels within the feature).
- D_{max} – Diameter (length) of the largest (longest) particle.
- D_{min} – Diameter (length) of the smallest (shortest) particle.
- L_p (perimeter) – The total length of the boundary of the feature. This is calculated from the horizontal and vertical projections, with an allowance for the number of corners.

- f_A (form area) – A shape factor of area. This is calculated from the ratio:

$$f_A = \frac{4A}{\pi \cdot D_{\text{max}} \cdot D_{\text{min}}} \text{ and for a circle and ellipse is equal to 1.}$$

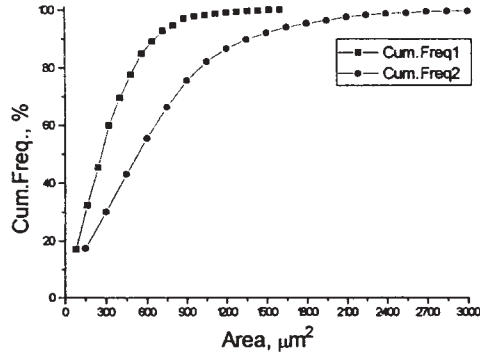


Fig. 1. Cumulative frequency as a function of area for not sieved powders.

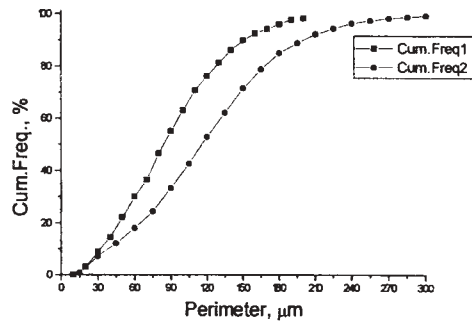


Fig. 2. Cumulative frequency as a function of perimeter for not sieved powders.

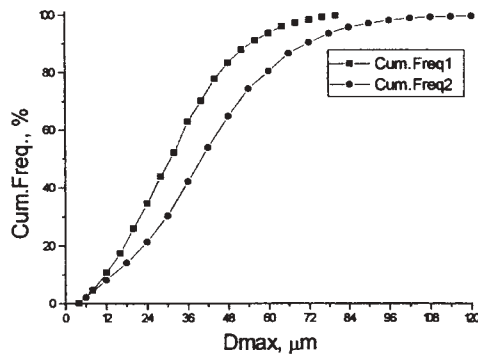


Fig. 3. Cumulative frequency as a function of D_{\max} for not sieved powders.

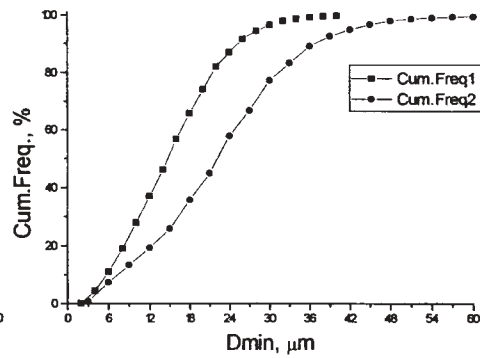


Fig. 4. Cumulative frequency as a function of D_{\min} for not sieved powders.

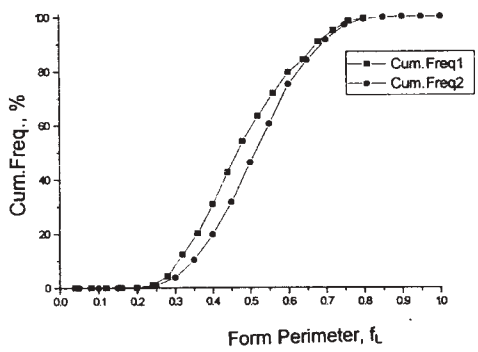


Fig. 5. Cumulative frequency as a function of form perimeter for not sieved powders.

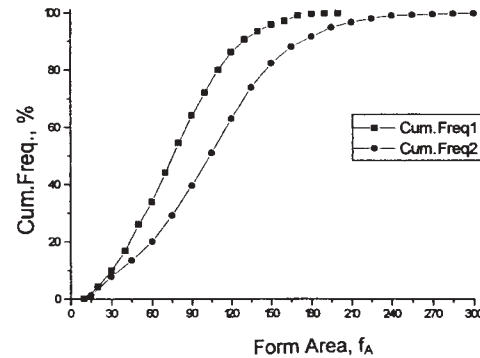


Fig. 6. Cumulative frequency as a function of form area for not sieved powders.

– f_L (form perimeter) – A shape factor of perimeter. This is calculated from the ratio:

$$f_L = \frac{4\pi A}{L_p^2} \text{ and for a circle and ellipse is equal to 1.}$$

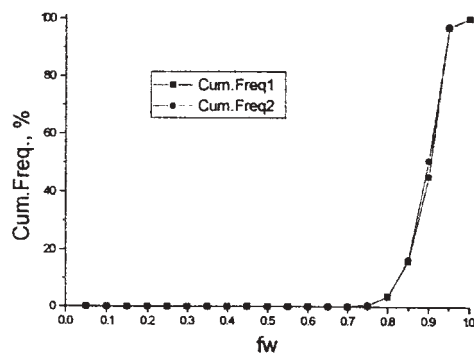


Fig. 7. Cumulative frequency as a function of f_w for not sieved powders.

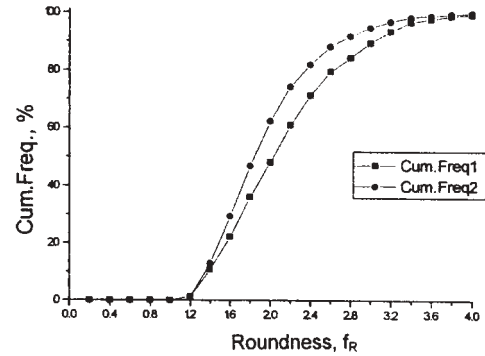


Fig. 8. Cumulative frequency as a function of roundness for not sieved powders.

– f_R (roundness) – A shape factor which gives a minimum value of unity for a circle. This is calculated from the ratio of perimeter squared to area:

$$f_R = \frac{L_p^2}{4\pi \cdot A \cdot 1.064}$$

The adjustment factor of 1.064 corrects the perimeter for the effect of the corners produced by the digitization of the image.

– f_w – This is the ratio of the length of the polygon circumscribing the feature formed by tangents to its boundary (very similar to the length of a piece of string stretched around the feature) to perimeter.

The difference in values of parameters which characterize the metal powders is obvious for non sieved powders obtained at different current densities. Because of this, the different dependences of the cumulative frequencies on the parameters can be seen in Figs. 1–8.

The same, but for the fraction (149–177) μm of both powders, is given in Tables III and IV, and Figs. 9–14.

TABLE III. The parameters which characterize the fraction (149–177) μm of powder I (apparent density 0.524 g/cm^3)

	Mean/ μm	Min/ μm	Max/ μm	RSE/%
$A(\text{area})/\mu\text{m}^2$	194.12	8.77	1256.52	1.84
L_p (perimeter)/ μm	67.61	0.93	270.20	1.14
$D_{\text{max}}/\mu\text{m}$	24.49	3.31	87.42	1.09
$D_{\text{min}}/\mu\text{m}$	11.93	1.99	43.71	1.07
f_A (form area)	0.76	0.31	1.00	0.44
f_L (form perimeter)	0.50	0.14	0.86	0.56
f_R (roundness)	2.04	0.48	6.70	0.62
f_w	0.90	0.67	0.97	0.15

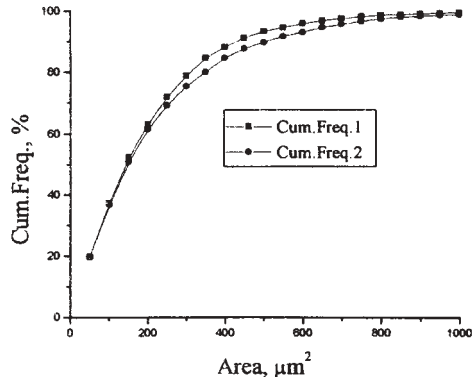


Fig. 9. Cumulative frequency as a function of area for sieved powders.

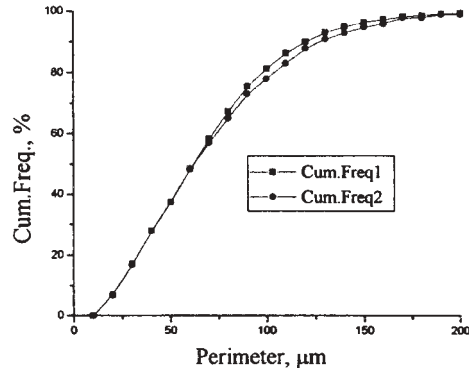


Fig. 10. Cumulative frequency as a function of perimeter for sieved powders.

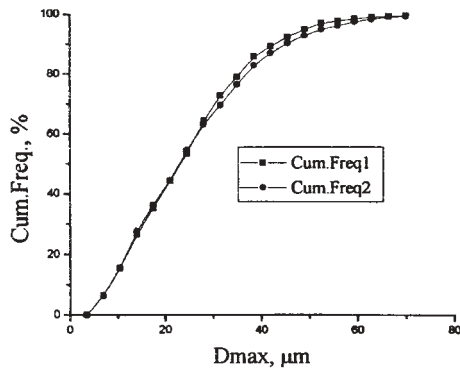


Fig. 11. Cumulative frequency as a function of D_{\max} for sieved powders.

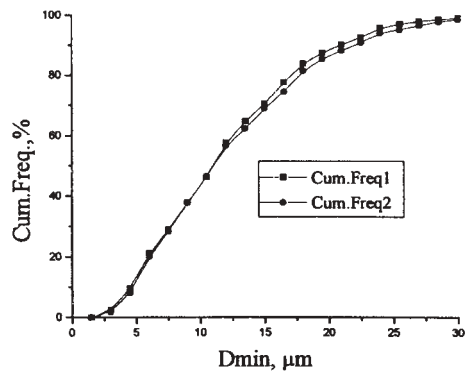


Fig. 12. Cumulative frequency as a function of D_{\min} for sieved powders.

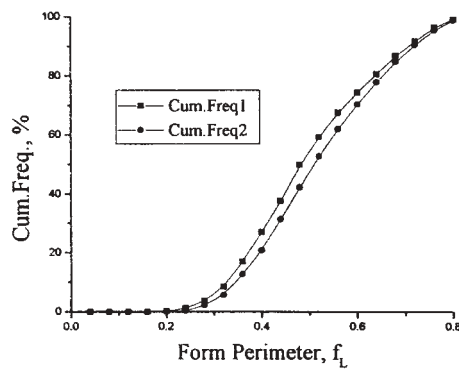


Fig. 13. Cumulative frequency as a function of form perimeter for sieved powders..

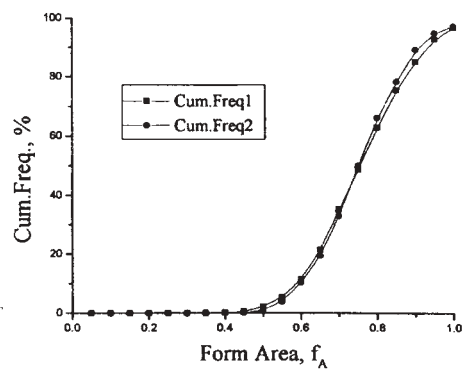


Fig. 14. Cumulative frequency as a function of form area for sieved powders.

In this case the values of all parameters are practically the same for the same fraction of both powders, producing practically one and the same dependence, but the values of apparent densities are still very different [fraction (149–177) μm , 0.524 g/cm³,

powder I; and fraction (149–177) μm , 1.122 g/cm^3 , powder II)]. Hence, all considered parameters do not affect the apparent density of copper powders. It should be also noted that the apparent densities of different fractions of powders are practically the same as illustrated by Tables V and VI.

TABLE IV. The parameters which characterize the fraction (149–177) μm of powder II (apparent density 1.122 g/cm^3)

	Mean/ μm	Min/ μm	Max/ μm	RSE/%
$A(\text{area})/\mu\text{m}^2$	216.30	8.98	2342.44	2.01
$L_p(\text{perimeter})/\mu\text{m}$	68.89	11.92	309.93	1.19
$D_{\text{max}}/\mu\text{m}$	25.11	3.43	98.01	1.16
$D_{\text{min}}/\mu\text{m}$	12.33	1.99	46.36	1.11
$f_A(\text{form area})$	0.75	0.38	1.00	0.41
$f_L(\text{form perimeter})$	0.52	0.17	0.87	0.52
$f_R(\text{roundness})$	1.94	1.08	5.39	0.58
f_w	0.91	0.76	0.97	0.11

TABLE V. Sieve analysis of granular copper powder I

Sieve designation/ μm	Apparent density/ g cm^{-3}	Time of flow/s
Not sieved	0.528	does not flow
Less than 74	0.716	39.5
74–88	0.578	32.0
88–149	0.532	26.0
149–177	0.524	does not flow
177–250	0.540	does not flow

TABLE VI. Sieve analysis of granular copper powder II

Sieve designation/ μm	Apparent density/ g cm^{-3}	Time of flow/s
Not sieved	1.838	does not flow
Less than 74	1.052	37.0
74–88	0.988	30.5
88–149	1.120	22.4
149–177	1.122	23.5
177–250	2.348	does not flow

The difference in apparent density can be explained by the analysis of the structure of the powder particles. SEM photomicrographs of powder I and II are presented in Figs. 15 and 16. By comparing Figs. 15 and 16 it is quite clear that the grain structure remains the

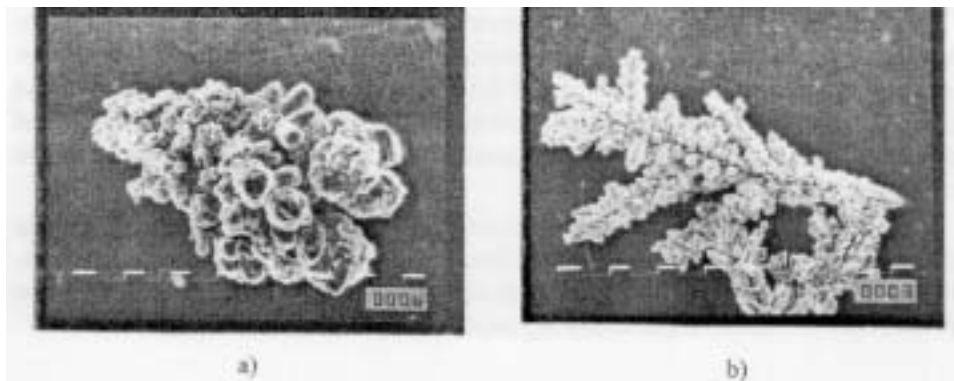


Fig. 15. SEM photomicrographs of copper powder particles obtained in constant current deposition. $c(\text{Cu}^{+2}) = 15 \text{ g/dm}^3$, $c(\text{H}_2\text{SO}_4) = 140 \text{ g/dm}^3$, $Q = 0.11 \text{ dm}^3/\text{min}$, $t = (50 \pm 2)^\circ\text{C}$, fraction less than $74 \mu\text{m}$, $\times 1500$ (a) $j = 1800 \text{ A/m}^2$, $\tau_r = 1.5 \text{ h}$, apparent density 1.052 g/cm^3 and (b) $j = 3600 \text{ A/m}^2$, $\tau_r = 15 \text{ min}$, apparent density 0.716 g/cm^3 .

same for both size ranges, *i.e.*, below $\approx 75 \mu\text{m}$ and above $\approx 150 \mu\text{m}$, respectively. In both size fractions two distinct shapes of the grains are present: one, more compact shown in Figs. 15a and 16a, characterized by small and more rounded dendrite branches, and the other one, shown in Figs. 15b and 16b, less compact, less rounded, characterized by more pronounced dendrite branching. They have well developed primary and secondary dendrite arms with the angles between them typical for the face centered cubic crystals.

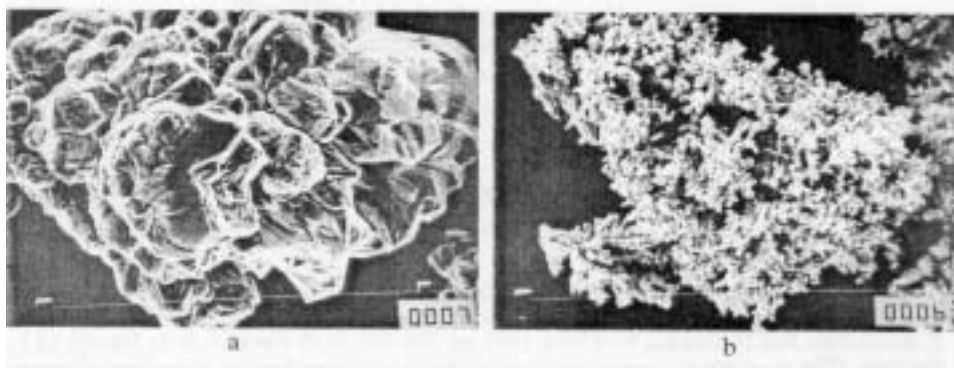


Fig. 16. SEM photomicrographs of copper powder particles obtained in constant current deposition. $c(\text{Cu}^{+2}) = 15 \text{ g/dm}^3$, $c(\text{H}_2\text{SO}_4) = 140 \text{ g/dm}^3$, $Q = 0.11 \text{ dm}^3/\text{min}$, $t = (50 \pm 2)^\circ\text{C}$, fraction $(149-177) \mu\text{m}$, $\times 1000$ (a) $j = 1800 \text{ A/m}^2$, $\tau_r = 1.5 \text{ h}$, apparent density 1.122 g/cm^3 and (b) $j = 3600 \text{ A/m}^2$, $\tau_r = 15 \text{ min}$, apparent density 0.524 g/cm^3 .

Obviously, the powder particles from the same fractions of different powders occupy approximately the same volume, but with considerably different structure of metallic copper. This causes the difference in apparent densities of copper powders obtained under different conditions, depending on the structure of electrodeposits. Obviously, the more dendritic is the structure of powder particles the smaller is the apparent density of copper powder.

It is known that more dendritic powder particles formation is enhanced by decreasing the concentration of deposition ions, increasing the concentration of the supporting electrolyte, increasing viscosity of the solution, decreasing the temperature and decreasing the circulation rate of the solution and *vice versa*. The apparent density of electrodeposited powders can hence be considerably changed by changing the above parameters as shown elsewhere.^{9–12}

On the other hand it was shown recently that the shape and structure of powder particles can be widely varied by using different regimes in electrodeposition at a periodically changing rate.² The effect of such regimes on the apparent density of copper powders will be treated in the following paper.

ИЗВОД

УТИЦАЈ СТРУКТУРЕ ЧЕСТИЦА НА НАСИПНУ МАСУ ЕЛЕКТРОЛИТИЧКИ ДОБИЈЕНОГ БАКАРНОГ ПРАХА

М. Г. ПАВЛОВИЋ¹, Љ. Ј. ПАВЛОВИЋ¹, Е. Р. ИВАНОВИЋ², В. РАДМИЛОВИЋ³ и К. И. ПОПОВ³

¹ИХТМ - Центар за електрохемију, Њеђошева 12, 11000 Београд, ²Пољопривредни факултет, Универзитет у Београду, Немањина 6, 11080 Земун - Београд и ³Технолошко-металуршки факултет, Универзитет у Београду, Карнегијева 4, 11000 Београд

Извршена је квалитативна микроструктурна и гранулометријска анализа бакарних прахова као и анализа морфологије и структуре честица праха помоћу скенирајуће електронске микроскопије (SEM). Установљено је да структура честица праха одређује насипну масу бакарног праха. Честице исте фракције различитих прахова заузимају отприлике исту запремину, али је структура металног бакра различита. Ово узрокује разлике у насипној маси бакарног праха добијеног под различитим условима. Што је структура честица више дендритична то је мања насипна маса бакарног праха.

(Примљено 6. јуна, ревидирано 30. августа 2001)

REFERENCES

1. R. M. German, *Powder Metallurgy Science*, 2nd ed., Metal Powder Industries Federation, Princeton, New Jersey, 1994, pp. 15–429
2. K. I. Popov, M. G. Pavlović, "Electrodeposition of metal powders with controlled particle grain size and morphology", in *Modern Aspects of Electrochemistry*, B. E. Conway, J. O'M. Bockris, R. E. White, Eds., Vol. 24, Plenum, New York, 1993, pp. 299–391; M. G. Pavlović, N. D. Nikolić, Lj. J. Pavlović, "The development, improvement and definition of electrochemical technology of copper powder production", Copper Smeltery and Refinery, Bor, 2000 (in Serbian)
3. M. G. Pavlović, K. I. Popov, E. R. Stojilković, *Bulletin of Electrochemistry*, **14** (1998) 211
4. ISO 3923-1979, ASTM B212
5. Lj. Radisavljević, M. G. Pavlović, N. D. Nikolić, I. D. Doroslovački, Č. Dumitrašković, *Powder Metallurgy, World Congress, Extended Abstracts*, Granada, Spain (1998), p. 121
6. ASTM B214-ISO 4497
7. R. T. De Hoff, F. N. Rhines, *Quantitative Microscopy*, Mac Graw Hill Book Comp., New York, 1968, p. 93
8. H. Modin, S. Modin, *Metallurgical Microscopy*, Butterworths, London, 1973, p. 143
9. N. Ibl, "The formation of powdered metal deposits", in *Advances in Electrochemistry and Electrochemical Engineering*, Vol. 2, Interscience, New York, 1962, pp. 50–55

10. A. Calusaru, *Electrodeposition of Metal Powders*, Elsevier, New York, 1979, pp. 352–355
11. A. R. Despić, K. I. Popov, “Transport controlled deposition and dissolution of metals” in *Modern Aspects of Electrochemistry*, Vol. 7, Plenum, New York, 1972, pp. 295–300
12. M. G. Pavlović, Lj. J. Pavlović, N. D. Nikolić, K. I. Popov, *Materials Science Forum* **352** (2000) 65–72.